

PACS numbers: 42.40.Eq; 78.20.Hp
DOI: 10.1070/QE2004v034n03ABEH002630

Use of reflection dynamic gratings for studying films and absorbing media

E.V. Ivakin, M. Ganjali, A.V. Sukhodolov, V.V. Filippov

Abstract. **Experimental studies are performed which demonstrate the use of dynamic gratings in a thin surface layer for investigations of the properties of solids strongly absorbing light. Methods are proposed for measuring the temperature conductivity χ of a gas adjacent to a surface and of a thin transparent film on the absorbing surface. The optical measurements of χ for porous silicon films on a substrate are performed.**

Keywords: *dynamic gratings, temperature conductivity, photoacoustics.*

1. Introduction

The method of pulsed dynamic gratings (DGs) [1] has a number of advantages over the known methods for studying and nondestructive control of materials based on photorefraction, photothermal, and optoacoustic phenomena. These advantages are due to the spatial periodicity of an excitation spot and the diffraction nature of the sample response to optical excitation. This method is versatile because gratings can be induced both inside a medium [2, 3] and on its surface [4]. The possibility to control the DG vector permits the separation of contributions from different mechanisms during the interaction of light with matter by analysing the amplitude, temporal, and phase characteristics of a diffracted beam.

The DG method has been widely applied in the last years for studying films and medium interfaces (see, for example, Refs [5 – 7]). The probing of gratings in reflected light substantially extends the field of applications of the DG method because strongly absorbing media can be studied. The use of reflection DGs produced by ultrashort laser pulses [8, 9] and of subgigahertz acoustic surface waves generated in this process proved to be quite efficient for studying the surface state. In this paper, we consider applications of DGs for measuring some physical parameters of an absorbing sample and a transparent medium in a thermal contact with the sample.

E.V. Ivakin, M. Ganjali, A.V. Sukhodolov, V.V. Filippov B.I. Stepanov Institute of Physics, National Academy of Sciences of Belarus, prosp. F. Skoriny 68, 220072 Minsk, Belarus; tel.: (1037517) 284 09 55; e-mail: ivakin@dragon.bas-net.by

Received 7 August 2003
Kvantovaya Elektronika **34** (3) 294 – 298 (2004)
Translated by M.N. Sapozhnikov

2. Experimental setup and samples

Experiments were performed using a setup similar to that described in Ref. [10]. DGs were recorded by the second harmonic of a Nd : YAG laser. The laser pulse duration and repetition rate were 12 ns and 10 Hz, respectively. The maximum energy density on the sample surface could achieve 0.1 J cm^{-2}, although experimental studies were mainly performed at energy densities no more than 0.05 – 0.07 J cm^{-2}, below the damage threshold of the sample surface. Because all the samples were opaque, the diffraction signal was observed in reflected light. DGs were probed by a beam from a synchronously modulated 30-mW He – Ne laser, which was incident on the sample at angles 45 – 60° with respect to the normal to the sample surface. The electric field vector lied in the plane of incidence, which was orthogonal to the grating vector. The DG spacing varied from 50 to 150 μm.

The amplitude calibration of the setup required for estimating the diffraction efficiency of DGs was performed using microsecond pulses from a He – Ne lasers and filters with the known transmission. This calibration can be used for diffracted light pulses of duration no less than 25 ns (the pulse response function width of the measuring system).

We studied the following samples in the form of plates polished from one side:

– Narrow-gap semiconductors: *n*-type (110)-cut silicon with the specific resistance of 20 Ω cm (the silicon surface was treated mechanically and chemically etched) and germanium with the mechanically treated surface. Except for specially indicated cases, samples were covered with a film of natural oxide of thickness no more than a few nanometres.

– Polycrystalline copper with a protective Al_2O_3 coating of thickness 450 nm.

– Porous silicon (PS) film of thickness 5 μm and porosity 50 % – 60 % on a crystalline Si substrate.

– Aluminium film of thickness 1 μm on a glass substrate.

Air (at different pressures) and organic liquids (ethanol and benzene) were used as transparent media in thermal contact with the surface. Samples were studied in a sealed chamber with a quartz window for input and output of optical radiation.

3. Results and discussion

Figure 1 shows a typical temporal behaviour of the diffracted light intensity for silicon in air (curve *1*) for the pump energy density $I = 0.06$ J cm^{-2}. Similar dependences

were obtained for germanium, polycrystalline copper, and an aluminium film on a glass substrate under the same experimental conditions. The replacement of air by liquid did not produce any qualitative changes in the diffraction type. Curve (*1*) demonstrates two decay processes: monotonic and oscillating. The first process is related to the formation of a thermal grating, while the second one is caused by excitation of acoustic waves in air. It is natural that the oscillations of the diffraction intensity are absent in vacuum [Fig. 1, curve (*2*)]. They are also absent for the PS film in air. The factors affecting the time dependence of diffraction are considered below.

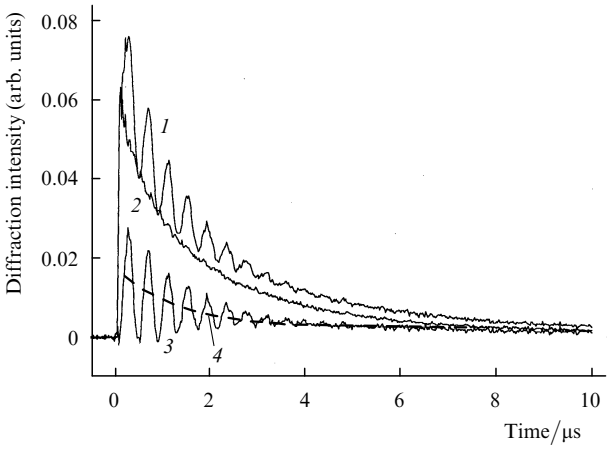

Figure 1. Diffraction kinetics for silicon in air (*1*) and vacuum at the residual pressure no more than 10^{-1} Torr (*2*); curve (*3*) is the difference of curves (*1*) and (*2*); curve (*4*) is a single exponential fit of curve (*3*), that describes the thermal component decay of diffraction in air. The grating period is 143 μm and the pump energy density is 0.06 J cm^{-2}.

3.1 Thermal grating on a surface

Upon optical excitation of the surface of a metal or a narrow-gap semiconductor, fast relaxation processes induce a thermal grating, which is strictly speaking the amplitude–phase grating. The amplitude component appears due to a temperature change in the surface reflectivity. The thermal reflection effect is being now extensively studied and is already used for the optical control of the surface temperature of solids [11, 12]. It was proposed in Ref. [13] to use the DG method for studying this effect, which can eliminate a number of problems in the optical-signal detection and improve the accuracy of measurements. The phase component of the DG appears due to the thermal expansion of a material and the formation of a relief on its surface.

Having the experimental data on the diffraction efficiency of a thermal grating at the instant of pulse termination, we can estimate the role of each component by comparing the data with calculations. The diffraction efficiency of the amplitude grating can be derived from [14] to give

$$D_{\text{ampl}} = \frac{1}{16} R_0 \left(\frac{\partial R}{\partial T} \frac{1}{R_0} \right)^2 \Delta T^2, \tag{1}$$

where R_0 and $(\partial R/\partial T)R_0^{-1}$ are the initial reflectivity and the temperature coefficient of its change for the probe beam; and ΔT is the amplitude of temperature modulation on the sample surface. Relation (1) is valid when variations in R are small compared to R_0, which is almost always fulfilled in experiments. For the relief (phase) grating, we have

$$D_{\text{ph}} = R_0 \left(\frac{\pi}{\lambda} \frac{\Delta h}{\cos \Theta} \right)^2, \tag{2}$$

where Δh is the total height of the relief on the surface and Θ is the inclination angle of the probe beam.

The average temperature increase in the surface layer of the sample produced to the end of a laser pulse of duration Δt can be estimated from the relation

$$\Delta T = \frac{E_0(1-r)}{c\rho l_{\text{therm}}}. \tag{3}$$

Here, E_0 is the surface energy density of the laser pulse; $c\rho$ is the heat capacity of the unit volume of a material; r is the reflectivity at the excitation wavelength;

$$l_{\text{therm}} = (4\Delta t \chi)^{1/2} \tag{4}$$

is the depth of a layer heated by the laser pulse during its action [6]; and χ is the temperature conductivity.

By using the tabulated values of χ for silicon, germanium, and copper, we obtain for a 12-ns laser pulse the values $l_{\text{therm}} = 1.9$, 1.1, and 2.3 μm, respectively. This gives, for the surface density of the absorbed energy $E_0(1-r)$ equal to 0.03 J cm^{-2}, the values of ΔT equal to 90, 120, and 40 K for the above materials, respectively. Because the coefficient $(\partial R/\partial T)R_0^{-1}$ for Si, Ge, and Cu is 1.5×10^{-4}, 2×10^{-4}, and 5×10^{-4}, respectively [14], it follows from (1) that the values of D_{ampl} for these materials are 0.6×10^{-3} %, 2.4×10^{-3} %, and 1.2×10^{-3} %, respectively.

Similar calculations for the relief grating using the relation

$$\Delta h = \alpha \frac{E_0(1-r)}{c\rho},$$

which is valid in the steady-state approximation (α is the thermal coefficient of linear expansion), give $\Delta h \approx 1$ nm for silicon and germanium and 1.5 nm for copper.

Thus, according to our calculations, the diffraction efficiency of the relief grating is $D_{\text{ph}} \approx 1.2 \times 10^{-2}$ % for silicon and germanium and $\sim 2.4 \times 10^{-2}$ % for copper. The experimental values of D_{ph}, which were measured, in particular, for Si and Ge, are $(0.6-0.8)\times 10^{-2}$ %, which is somewhat lower than calculated values. Therefore, the thermal relief grating makes the main contribution to the diffraction signal. The energy dependence of the initial diffraction efficiency of the thermal DG is quadratic (Fig. 2), in accordance with the accepted physical concepts.

Note for completeness that, along with comparatively slow thermal processes proceeding upon excitation of silicon and germanium surfaces, we observed a short diffraction pulse, whose duration was shorter than the width of the pulse characteristic of the detection system. For the excitation energy density exceeding 0.08 J cm^{-2}, the pulse amplitude was several times greater than the initial amplitude of diffraction from the thermal surface grating. A similar diffracted pulse of duration 0.5 ns was observed earlier upon picosecond [8] and femtosecond [9] excitation,

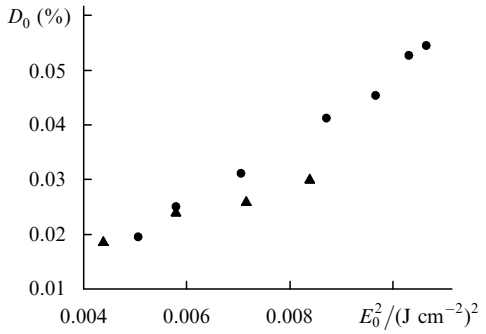

Figure 2. Energy dependences of the initial diffraction efficiency D_0 of the thermal grating on the surface of silicon (●) and germanium (▲) in air.

although the mechanism of its formation was not discussed. A strong diffraction is explained by the formation of a periodic relief on a semiconductor surface due to the electron-deformation interaction of photoexcited carriers with a crystal lattice [15–17].

The kinetics of light diffraction from the thermal grating can be used to determine the temperature conductivity of materials with strong surface absorption. In this case, to exclude the influence of the air layer adjacent to the heated surface on the results of measurements, this parameter should be measured in a vacuum chamber. It was shown in Refs [6, 18] that the decay of the thermal relief on the thermally insulated absorbing interface is described by the error function $\mathrm{erfc}(t/\tau)^{1/2}$, where $\tau = \Lambda^2/(4\pi^2\chi)$, and Λ is the grating period. In our case, the fit of the experimental dependences of diffraction from a sample by the function

$$D_s(t) = D_s(0)\mathrm{erfc}^2\left(\frac{4\pi^2\chi t}{\Lambda^2}\right)^{0.5} \quad (5)$$

within the time window corresponding to the change in the diffraction signal from 0.95 to 0.1 of its maximum value, where distortions and noise are small, gives a satisfactory agreement with the tabulated values of χ for silicon, germanium, and copper. In particular, the temperature conductivity of a silicon plate, measured at its different points, lies in the range between 0.57 and 0.62 $\mathrm{cm^2\ s^{-1}}$. In contrast to this, a similar procedure for an aluminium film ($\chi \approx 1\ \mathrm{cm^2\ s^{-1}}$) on a glass plate ($\chi \approx 6 \times 10^{-3}\ \mathrm{cm^2\ s^{-1}}$) gives the value $\chi = 0.04 - 0.05\ \mathrm{cm^2\ s^{-1}}$, which can be considered only as the effective value for the metal film–glass system.

The nature of diffraction in the PS film is different. For the porosity indicated above (50 %–60 %), the film is virtually transparent for radiation of a He–Ne laser due to the shift of the edge of the fundamental absorption band caused by the size quantisation effect. At the same time, absorption at the pump wavelength is comparatively strong [19]. The heat release in the film results in the formation of a bulk refractive-index grating. Since the data on $\mathrm{d}n/\mathrm{d}T$ for PS were not available to us, we used the value of the temperature coefficient for crystalline silicon equal to $10^{-4}\ \mathrm{K^{-1}}$ [20]. This gives the diffraction efficiency of a layer of the order of a few percent for pumping used in experiments. At the same time, due to a low energy deposition to the surface of silicon, the relief grating is inefficient. Because the effusion coefficients for porous and single-crystal silicon are substantially different, the role of a substrate in the kinetics of the grating decay is negligible. This is confirmed by the fact that the detected lifetime of the DG in porous silicon is 40–50 times longer and, hence, it is mainly determined by the thermal properties of the film.

The experimental decays of diffraction for the PS film in vacuum better correspond to the exponential law. This is explained by the fact that, according to the above comments, the formation of the diffracted signal is mainly determined by the bulk phase grating in the film, whereas the influence of the substrate is weak. Our measurements showed that the temperature conductivity of PS lies in the range between 0.016 and 0.020 $\mathrm{cm^2\ s^{-1}}$ for a freshly prepared sample and in the range from 0.010 to 0.012 $\mathrm{cm^2\ s^{-1}}$ for a sample kept for 15 days in the open atmosphere. Such a variation in χ can be explained by the condensation of water in film pores and the filling of pores by silicon dioxide due to natural oxidation. The presented values of χ correspond to the data obtained for nanostructured PS films by the methods of photoacoustic spectroscopy [21].

3.2 Thermal effects in the boundary layer in gases and liquids

A small fraction of thermal energy released at the absorbing surface is transferred to the adjacent layer of a transparent medium, resulting in the production of a thermal grating and an acoustic wave in the layer (if the conditions presented below are satisfied). The efficiency of thermal excitation of a transparent layer in contact with the heated surface was considered many times in earlier papers devoted, in particular, to the mirage method (see, for example, Ref. [22]). According to Ref. [6], the coefficient γ of thermal coupling between adjacent media is described by the expression

$$\gamma = \frac{\varepsilon_{g,l}}{\varepsilon_s + \varepsilon_{g,l}} \cong \frac{\varepsilon_{g,l}}{\varepsilon_s},$$

where $\varepsilon = c\rho\sqrt{\chi}$ is the effusion of gas (g), liquid (l) or a solid sample (s).

Table 1 presents the values of γ for interfaces studied. It also contains the data required for the approximate estimates of the diffraction efficiency of the thermal grating in air and organic liquids for the surface density of absorbed energy equal to 0.03 J $\mathrm{cm^{-2}}$. The values of I_{therm} and ΔT for transparent layers were calculated from relations (3) and (4) taking into account the corresponding coefficients of thermal coupling. The initial values of D_{ph} of the phase grating for transparent layers were calculated, using the temperature coefficients of the refractive index equal to $\mathrm{d}n/\mathrm{d}T = -10^{-6}$, -4×10^{-4} and $-6.5 \times 10^{-4}\ \mathrm{K^{-1}}$ for air, ethanol, and benzene, respectively, from expression in which Δh, determining the phase shift, was replaced by $\Delta n\, l_{\mathrm{therm}}$.

Table 1.

Interface	$\gamma/10^{-3}$	$l_{\mathrm{therm}}/\mu\mathrm{m}$	$\Delta T/\ \mathrm{K}$	$D_{\mathrm{ph}}(10^{-4}\ \%)$
Air–copper	0.16	0.9	35	0.03
Air–silicon	0.32	0.9	80	0.14
Air–germanium	0.62	0.9	150	0.6
Ethanol–silicon	19	0.07	5	0.4
Benzene–silicon	26	0.06	7	1.8

One can see from Table 1 that the diffraction efficiency of the transparent boundary layer is more than two orders of magnitude lower than the diffraction efficiency of the thermal grating on the surface of silicon, germanium, and copper samples. Nevertheless, experimental curve (*1*) (Fig. 1) exhibits acoustic oscillations and, hence, the corresponding thermal component is present in air as well. In our opinion, such a low-efficient grating can be observed because of the heterodyne amplification of a weak field due to the presence of a comparatively high-power diffraction beam on the thermal surface grating. The amplification occurs because both coherently interacting diffraction fields from two thermal gratings are in phase with each other. It is because these fields are in phase, curve (*1*) in Fig. 1 being located above curve (*2*).

By using the results obtained in Ref. [2], we write the equation for the total diffraction efficiency of the thermal grating taking into account heterodyning and the smallness of the signal from the thermal grating in the medium adjacent to the sample:

$$D_\Sigma(t) \simeq D_s(0) f_1^2(t) + 2[D_s(0) D_{g,l}(0)]^{1/2} f_1(t) f_2(t). \qquad (6)$$

Here, for all samples except PS, the time functions have the form $f_1 = \mathrm{erfc}(t/\tau_s)^{1/2}$ and $f_2 = \exp(-t/\tau_{g,l})$. For PS, $f_1 = \exp(-t/\tau_s)$ because of the bulk type of the DG.

We can assume in estimates that the heterodyne gain is equal to the doubled root from the ratio of the diffraction intensities for the sample and medium. For silicon and germanium, for example, in air, the amplification of the diffraction signal from the thermal grating in air at the initial instant of time is ~ 60 and 30, respectively.

Figure 1 also shows curve (*3*), which is the difference of two signals detected successively in the presence of air in a chamber with the sample and in the evacuated chamber. We used the difference curves, described by the second term in (6), to find the function $f_2(t)$ by fitting and then to estimate the possibility of determining the temperature conductivity of air from the found value of τ_g. The fitting was performed for a finite region of the difference curve, where the influence of acoustic oscillations was weaker. The value of τ_s for a sample was taken from the time dependence obtained in vacuum.

We compared the results of our calculations with the data obtained by other authors. According to Refs [23, 24], the temperature conductivity of air at the normal pressure increases linearly from $0.15\ \mathrm{cm^2\ s^{-1}}$ at 300 K to $0.45-0.47\ \mathrm{cm^2\ s^{-1}}$ at 400 K. As follows from Table 1, our measurements of the silicon–air system were performed at the volume-averaged air temperature equal to ~ 380 K. We found that the temperature conductivity was $0.32-0.42\ \mathrm{cm^2\ s^{-1}}$. It seems that a great scatter in the results obtained and somewhat understated values of χ compared to the tabulated values are explained by the influence of noise and the dependence of the fitting results on the reliability of measuring τ_s. In addition, the real temperature of air during measurements can differ from the values presented above.

3.3 Acoustic waves in the boundary layer

The oscillating component in Fig. 1 is related to the thermal excitation of two acoustic waves in the adjacent transparent layer at the frequency ν, which propagate at the velocity $V = \Lambda\nu$ in the opposite directions along the grating vector. Figure 3 shows the experimental dependence of the amplitude of the acoustic diffraction signal on the air pressure in a chamber with silicon. One can see that this dependence is close to linear in this pressure range, although according to Ref. [6], the amplitude of oscillations is determined by a number of parameters depending on the gas pressure, including the thermal coefficient of variation in the refractive index, effusion, density, and sound speed.

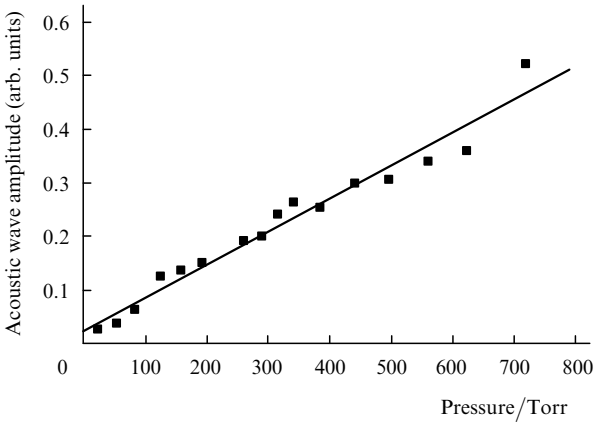

Figure 3. Dependence of the initial amplitude of the acoustic wave on the air pressure in a chamber. The absorbing surface is crystalline silicon.

We found also that the presence of the SiO_2 film grown on the silicon surface reduces the amplitude of acoustic waves in air and causes the phase delay of oscillations of the diffraction signal. In particular, as the film thickness h increases from 100 to 440 nm (other conditions being the same), the amplitude of the acoustic wave in air decreases approximately by half, and the phase delay of the oscillating signal becomes equal to 1.43 rad, which, for the grating period equal to 144 μm, corresponds to the time delay ~ 100 ns.

The amplitude of the acoustic wave decreases, in particular, due to the broadening of a thermal pulse propagating from the film-absorbing medium interface to the film–air interface. It was shown already in earlier papers (see, for example, Ref. [25]) that the amplitude of oscillations is determined by the convolution of the heating pulse function with the function describing a travelling acoustic wave. In this situation, the time factor, depending on the relation between the oscillation period p and the heating pulse duration τ_h, plays a substantial role. For a Gaussian thermal pulse, the change η_2/η_1 in the efficiency of excitation of an acoustic wave in a medium when the film thickness increases from h_1 to h_2 can be estimated from the expression [6]

$$\frac{\eta_2}{\eta_1} = \exp\left(-2\pi^2 \frac{\tau_{h_2}^2 - \tau_{h_1}^2}{p^2}\right). \qquad (7)$$

We assume below that the duration of a thermal pulse heating an air layer is approximately equal to the transit time for heat from the film–substrate interface to the film–air interface. For the above-mentioned film thicknesses and $\chi_{SiO_2} = 6 \times 10^{-3}\ \mathrm{cm^2\ s^{-1}}$, the pulse durations $2\tau_{h_1}$ и $2\tau_{h_2}$ found from expression (4) in which Δt was replace by $2\tau_{hi}$, are equal to 4 and 77 ns, respectively. For $p = 440$ ns, the ratio $\eta_2/\eta_1 = 0.85$. The difference by a factor of 1.7 from

the experiment value is probably explained by the deviation of the thermal pulse shape from a Gaussian. As for the phase shift, the calculated and experimental values are in agreement within 15 %. This means that the film thickness can be determined from phase measurements if its temperature conductivity is known or, vice versa, the value of χ can be found for a film with the known thickness along the normal to the sample.

For copper with the Al_2O_3 film under the same experimental conditions, oscillations of the diffracted signal are barely noticeable. The data presented in Table 1 and calculated values of γ show that this is mainly explained by inefficient heat transfer from copper to air through the Al_2O_3 film, whereas the film itself almost does not affect the efficiency of the thermoacoustic coupling. In the diffraction kinetics for a comparatively thick PS film, no acoustic waves in air was detected at all, which is caused by a strong (compared to the SiO_2 and Al_2O_3 films) broadening of a pulse heating gas.

When the camber with samples was filled with liquids, the kinetic curves were observed, which were similar to those shown in Fig. 1 but with higher-frequency oscillations in the range from 10 to 20 MHz. The ultrasonic speeds in benzene and ethanol measured in experiments coincide within 10 % with their tabulated values. The amplitude of acoustic oscillations noticeably decreased with decreasing the grating period. This is explained by a stronger influence of the oscillation period p [see expression (7)], which is approximately three times smaller for liquids compared to air for the same Λ.

4. Conclusions

Surface dynamic gratings probed in reflected light extend the field of applications of the DG method to materials opaque for exciting radiation and allow the measurement of the temperature conductivity in the boundary region of samples along the surface to be performed (if the sample boundary is thermally insulated).

The heterodyne amplification of the light field caused by diffraction from the relief grating provides the detection of a signal from the thermal DG in a thin gas layer down to the diffraction efficiency of 10^{-4} %. The difference curve of the diffraction decay allows the measurement of the temperature conductivity of gases and liquids transparent in the spectral region of light used in experiments. This requires the knowledge of the thermal properties of the sample material.

Our studies have shown that phase measurements can be used to determine the temperature conductivity of transparent films with the known thickness on an absorbing substrate along the normal to its surface. When transparent media are used in which the sound speed is greater than in gases, for example, liquids, the sensitivity of measurements increases and, hence, the DG method can be applied for studying thinner films.

Acknowledgements. This work was supported by the Belarussian Committee of Science and Technology (Grant No. M-20).

References

1. Eichler H.J., Günter P., Pohl D.W. *Laser-induced Dynamic Gratings* (Berlin, Heidelberg, New York, Tokyo: Springer-Verlag, 1986).
2. Pohl D.W. *IBM J. Res. Develop.*, **23** (5), 604 (1979).
3. Nagasaka Y., Hatakeyama T., Okuda M., Nagashima A. *Rev. Sci. Instrum.*, **59**, 1156 (1988).
4. Cachier G. *Appl. Phys. Lett.*, **17**, 419 (1970).
5. Duggal A.R., Rogers J.A., Nelson K.A. *J. Appl. Phys.*, **72**, 2823 (1992).
6. Zhang B., Imhof R. *Proc. Roy. Soc. Lond. A*, **456**, 2781 (2000).
7. Ivakin E.V., Rubanov A.S. *Analytical Sci.*, **17**, 126s (2001).
8. Sawada T., Harata A. *Appl. Phys. A*, **61**, 263 (1995).
9. Morishita T., Hibara A., Sawada T., Tsuyumoto I. *Analytical Sci.*, **16**, 403 (2000).
10. Ivakin E.V. *Opt. Zh.*, **67**, 27 (2000).
11. Rosencwaig A., Opsal J., Smith W.L., Willenborg D.L. *Phys. Lett.*, **46**, 1013 (1985).
12. Magunov A.N. *Lazernaya termometriya tverdykh tel* (Laser Thermometry of Solids) (Moscow: Fizmatlit, 2002).
13. Imhof R.E. UK Patent 6 2224835A. Int. cl. G01N 21/47 (1990).
14. Alekseev-Popov A.V. *Zh. Tekh. Fiz.*, **47**, 1986 (1977).
15. Tucker J.W., Rampton V.W. *Microwave Ultrasonics in Solid State Physics* (Amsterdam, North Holland, 1972; Moscow: Mir, 1975).
16. Avanesyan S.M., Gusev V.E., Zheludev N.I. *Appl. Phys. A*, **40**, 163 (1986).
17. Chigarev N.V., Parashchuk D.Yu., Pan Yu.S., Gusev V.E. *Zh. Eksp. Teor. Fiz.*, **121**, 728 (2002).
18. Käding O.W., Skurk H., Maznev A.A., Matthias E. *Appl. Phys. A*, **61**, 253 (1995).
19. Strashnikova M.I., Voznyi V.L., Reznichenko V.Ya., Gaivoronskii V.Ya. *Zh. Eksp. Teor. Fiz.*, **120**, 409 (2001).
20. Eichler H.J., Massmann F., Biselli E., Richter K., Glotz M., Kometzke L., Yang X. *Phys. Rev. B*, **36**, 3247 (1987).
21. *Properties of porous silicon. Datareview*, series No18 (London: INSPEC, 1977, §4.3).
22. Murphy J.C., Aamodt L.C. *J. Appl. Phys.*, **51**, 4580 (1980).
23. Vargaftik N.B. *Spravochnik po teplofizicheskim svoistvam gazov i zhidkostei* (Handbook of Thermal Properties of Gases and Liquids) (Moscow: Fizmatgiz, 1963).
24. Yun S.I., Ki-Dong Oh, Kwon-Sang Ryu, Chang-Geon Kim, Park H.L., Seo H.J. *Appl. Phys. B*, **40**, 95 (1986).
25. Ivakin E.V., Lazaruk A.M., Petrovich I.P., Rubanov A.S. *Kvantovaya Elektron.*, **4**, 2421 (1977) [*Sov. J. Quantum Electron.*, **7**, 1382 (1977)].